

Temperature dependence of the effective anisotropies in magnetic nanoparticles with Néel surface anisotropy

This article has been downloaded from IOPscience. Please scroll down to see the full text article.

2010 J. Phys. D: Appl. Phys. 43 474009

(<http://iopscience.iop.org/0022-3727/43/47/474009>)

View [the table of contents for this issue](#), or go to the [journal homepage](#) for more

Download details:

IP Address: 144.32.126.16

The article was downloaded on 15/11/2010 at 10:33

Please note that [terms and conditions apply](#).

Temperature dependence of the effective anisotropies in magnetic nanoparticles with Néel surface anisotropy

R Yanes¹, O Chubykalo-Fesenko¹, R F L Evans² and R W Chantrell²

¹ Instituto de Ciencia de Materiales de Madrid, CSIC, Cantoblanco, 28049 Madrid, Spain

² Department of Physics, University of York, Heslington, York YO10 5DD, UK

Received 21 May 2010, in final form 27 July 2010

Published 11 November 2010

Online at stacks.iop.org/JPhysD/43/474009

Abstract

We discuss the physical concept of the effective anisotropy in magnetic nanoparticles with surface anisotropy. A recently developed constrained Monte Carlo method allows evaluation of the temperature dependence of the energy surface in the whole temperature range, from which the effective anisotropy is determined. We consider nanoparticles of different shapes with cubic or uniaxial core anisotropy and Néel surface anisotropy. We demonstrate that at low temperatures surface effects can be dominant, leading to an overall cubic effective anisotropy even in spherical nanoparticles with uniaxial core anisotropy. This cubic anisotropy contribution decreases more rapidly with increasing temperature than the uniaxial core anisotropy, leading to a temperature-induced reorientation transition. We discuss the scaling behaviour of the effective anisotropy with magnetization in nanoparticles with surface anisotropy contribution. The scaling exponent deviates from that expected from Callen–Callen theory due to increased fluctuations of the surface spins.

(Some figures in this article are in colour only in the electronic version)

1. Introduction

The surface functionalization of nanoparticles is one of the most important challenges in their synthesis. Different chemical surface engineering techniques can be used to develop a wide range of functional properties, including magnetic [1, 2].

In general terms, the magnetic behaviour of nanoparticles is strongly influenced by their surface properties due to a high surface-to-volume ratio [3]. Specific magnetic properties required for technological applications generally depend on the magnetic thermal stability, i.e. on the blocking temperature, defined by the relevant magnetic energy barrier between stable magnetic states. The magnetic energy barrier is proportional to the nanoparticle size and the magnetic anisotropy value. Magnetic nanoparticles with different shapes also show different magnetic properties (including energy barriers) due to a shape anisotropy arising from the magnetostatic field [4, 5]. Additionally, it is also possible to control the energy barrier by modification of the surface, for example, oxidation of the nanoparticle may increase the

energy barrier via the exchange-bias effect [6, 7]. Magnetic nanoparticles embedded in non-magnetic matrices, such as Co in Au, Ag, or Cu, have also been reported to exhibit an increased blocking temperature [8–10]. The engineering of the energy barrier of magnetic nanoparticles is important for their possible applications in magnetic recording [6, 11]. The combination of materials with different magnetic properties (as in the core-shell nanoparticles) also allows the control of energy barriers almost independently of the coercive field [7, 12, 13].

Magnetic surface effects manifest themselves in multiple ways including, but not limited to, the lack of crystallographic symmetry on the surface [14], expansion or contraction of the lattice structure [15, 16], reduction in coordination number, roughness, spin–orbit interaction and charge transfer phenomena [10, 17]. In practice, it is impossible to separate these effects and consequently, all of them are normally embedded in a phenomenological concept of the ‘surface anisotropy’. Experimentally, it is customary to characterize the surface anisotropy via size-dependent measurements of the relevant energy barrier. The surface anisotropy is then

calculated from a formula [18], which has become a central feature in the study of magnetic nanoparticles [1, 3, 8, 9, 19, 20]. The phenomenological formula reads

$$K_{\text{eff}} = \Delta E/V = K_V + \frac{K_{\text{Surf}}}{D}, \quad (1)$$

where D is the nanoparticle diameter and K_{Surf} is the ('effective') surface anisotropy. ΔE is the relevant energy barrier, determined, for example, using ac-susceptibility measurements, and K_V is the effective bulk anisotropy. The relationship to the energy barrier depends on the anisotropy type, specifically, for uniaxial anisotropy $K_V = K_C$ and for cubic anisotropy $K_V = K_C/4$ if $K_C > 0$ or $K_V = |K_C|/12$ if $K_C < 0$, where K_C is the core magnetocrystalline anisotropy. The value of K_{Surf} is normally extracted experimentally via the linear plot of K_{eff} as a function of $1/D$. Clearly the understanding of the meaning of the term 'effective' anisotropy in some model situations is important.

A detailed theoretical description of the real experimental situation is almost impossible due to competition between many effects and large dispersion of individual nanoparticle properties. Additionally, the full quantum mechanical treatment of a 10 nm nanoparticle is still not feasible. From the theoretical point of view, the quantum mechanical description is limited to small clusters only [21, 22] and cannot fully take into account the effects of spin non-collinearity, spin dynamics and temperature.

The so-called 'atomistic' description [23–26] is based on the Heisenberg-type Hamiltonian and can include spin dynamics and temperature. As a disadvantage, these calculations use phenomenological surface anisotropy models, such as the transverse anisotropy [27]. One of the most justified models for the surface anisotropy is the widely used Néel surface anisotropy model [23, 28, 14] which will be also used in this paper. It should be noted that the Néel surface anisotropy model comes from the magnetostriction effect due to the lack of crystallographic symmetry on the surface [28, 14]. An attempt to justify the model from a quantum mechanical approach currently exists only for thin films [29]. Nevertheless, it is the most reasonable phenomenological model which takes into account the different strengths of the anisotropy for surface atoms with differing local environments.

Recent theoretical works [23, 24, 30] using the Néel surface anisotropy model (with the surface anisotropy parameter K_s) have shown that strong surface anisotropy generally leads to spin non-collinearities. The main effect is the change of the effective magnetic energy landscape of a nanoparticle, leading to the appearance of an additional cubic anisotropy ($\sim K_s^2$) in nanoparticles with uniaxial core anisotropy [23]. Among other effects, this destroys the applicability of the formula (equation (1)) in nanoparticles with symmetric shapes such as spherical or truncated octahedral nanoparticles [24].

In elongated nanoparticles, such as ellipsoidal or elongated truncated octahedra [23, 24, 31], an additional uniaxial anisotropy ($\sim K_s$) appears. Then there are two cases

when the additional anisotropy due to the surface effect has the same nature as the core anisotropy and is additive in the spirit of formula (1): (i) elongated nanoparticles with uniaxial core anisotropy and negative surface anisotropy, (ii) spherical nanoparticles with cubic core anisotropy and positive surface anisotropy. However, even in these cases, the effective anisotropy K_{Surf} does not coincide with the Néel surface anisotropy value K_s since the averaging of the magnetization over the surface spins should be taken into account [24, 31]. Since formula (1) is not valid, one cannot separate the surface contribution from the bulk one and only the notion of the total 'effective' anisotropy remains [24, 31]. The fit of the experimental data avoiding the use of this formula (1) shows very large values of the surface anisotropy K_s up to values of the order of the exchange parameter for Co nanoparticles capped with Au [31].

The appearance of an additional cubic anisotropy contribution due to surface effects is an important manifestation of the surface anisotropy concept. Unfortunately it is difficult to demonstrate it in measurements on an ensemble of magnetic nanoparticles where different internal structures could coexist. It has been suggested that the additional cubic anisotropy contribution could potentially be traced in measurements on individual nanoparticles using micro-SQUID as well as in ensemble of nanoparticles using ferromagnetic resonance (FMR) [33]. It should be noted that for complex energy landscapes, the use of the energy barrier as the definition of the 'effective anisotropy' adds an additional complexity [23, 24], since in the presence of the two contributions, the energy barriers cannot be evaluated as a simple expression $K_{\text{eff}}V$. In this case, more complex studies such as the angular dependence of the switching fields are more useful [14, 32].

The above mentioned effects show the necessity to understand different contributions to the 'effective' anisotropy in nanoparticles as multi-spin systems. Up to now the concept of the additional cubic anisotropy due to surface effects in magnetic nanoparticles has been demonstrated at zero-temperature only, but rigorously taking into account the spin non-collinearities. In this paper we introduce temperature effects in the evaluation of the effective anisotropy in individual nanoparticles. It is reasonable to ask the question; what happens to these effective anisotropies with additional spin non-collinearities due to thermal disordering. A recently developed constrained Monte Carlo (CMC) method [34] allows the evaluation of effective anisotropies in nanoparticles as multi-spin systems for arbitrary temperature. In this paper we apply the CMC method to evaluate the temperature dependence of both uniaxial and cubic anisotropy contributions in nanoparticles of different shapes, core anisotropy and cut from different crystal lattices. We show that interesting phenomena can occur in magnetic nanoparticles due to the surface anisotropy contribution, such as a magnetization reorientation transition, an effect similar to that occurring in thin films. We also show that the surface, being more sensitive to temperature fluctuations, influences the scaling behaviour of the effective anisotropy with magnetization.

2. Model

In this paper we consider truncated octahedra and spherical Co nanoparticles cut from simple cubic (sc) or face-centred cubic (fcc) crystal structure. We also consider nanoparticles of two sizes which for Co parameters would correspond to diameters $D \approx 3$ nm (approximately 1200–1500 atoms, depending on the underlying lattice and the shape) and $D \approx 7.8$ nm (approximately 6300 atoms for a spherical nanoparticle with sc lattice). To model the magnetic behaviour we use a classical atomistic spin model with Heisenberg exchange. The total magnetic energy is written as

$$\mathcal{H} = -\frac{1}{2}J \sum_{i,j}^N \vec{s}_i \vec{s}_j + E_{\text{ani}}, \quad (2)$$

where J is the nearest-neighbour exchange energy (for Co we use $J = 1.0 \times 10^{-13}$ erg for sc and $J = 5.6 \times 10^{-14}$ erg for fcc lattices), \vec{s}_i is the localized spin moment ($|\vec{s}_i| = 1$), N is the number of spins in the particle and E_{ani} is the anisotropy energy. For core spins, we use the magnetocrystalline anisotropy in the uniaxial form:

$$E_{\text{ani}}^{\text{uni}} = -K_c \sum_i^{N_c} s_{i,z}^2, \quad (3)$$

or in the cubic form

$$E_{\text{ani}}^{\text{cub}} = -\frac{1}{2}K_c \sum_i^{N_c} (s_{i,x}^4 + s_{i,y}^4 + s_{i,z}^4), \quad (4)$$

where K_c is the core anisotropy value ($K_c = 4.16 \times 10^6$ erg cm $^{-3}$) and N_c is the number of core spins. In the uniaxial case the anisotropy is assumed to be directed parallel to the z direction while in the cubic case the three anisotropy axes are directed along the coordinate axes x , y , z . For surface spins (with less than the full coordination number) we use the Néel surface anisotropy model [28, 14]:

$$E_{\text{ani}}^{\text{NSA}} = \frac{K_s}{2} \sum_i^{N_s} \sum_j^{z_i} (\vec{s}_i \vec{u}_{ij})^2. \quad (5)$$

Here K_s is the Néel surface anisotropy magnitude, N_s is the number of surface spins, z_i is the coordination number of spin i and \vec{u}_{ij} is the unit vector connecting the spin i with its nearest neighbour j .

To evaluate the effective energy landscapes at $T = 0$ K in a multi-spin particle, we use the Lagrangian multiplier method [5, 23, 24, 30]. Briefly, in the case of nanoparticles with surface anisotropy dominated by the exchange interactions [23, 24, 14], one can expect the global behaviour corresponding to the rotation of the particle macro-spin as a whole. The numerical procedure then considers the multidimensional space projected into one unit magnetization vector $\vec{m}_0(\theta, \varphi)$. This is done by adding an additional term $-N\bar{\lambda}(\vec{m} - \vec{m}_0)$ to the total energy, where $\bar{\lambda}$ is the Lagrangian multiplier, $\vec{m} = \sum \vec{s}_i / |\sum \vec{s}_i|$ is the particle magnetization direction and \vec{s}_i are the individual local magnetic spins. This term produces an additional constraint field forcing the net magnetization along

the direction $\vec{m}_0(\theta, \varphi)$, while fully allowing local deviations from the collinear magnetization state. To find the conditional minimum, the Landau–Lifshitz–Gilbert equation of motion without the precessional term is solved.

$$\frac{d\vec{s}_i}{dt} = -\alpha[\vec{s}_i \times [\vec{s}_i \times \vec{h}_i]], \quad (6)$$

where α is the formal damping parameter, $\vec{h}_i = -\partial\mathcal{E}/\partial\vec{s}_i$ is the local field and $\mathcal{E} = \mathcal{H} - N\bar{\lambda}(\vec{m} - \vec{m}_0)$ is the total system magnetic energy augmented with the Lagrangian multiplier term. To these equations one should also add three equations for the Lagrangian multiplier components: $\dot{\bar{\lambda}} = \partial\mathcal{E}/\partial\bar{\lambda}$. The stationary points found in this approach are also the stationary points of the original Hamiltonian. The method can evaluate non-collinear multidimensional stationary points in the multi-spin space.

The method allows the calculation of effective energy landscapes for a nanoparticle in terms of the constraint direction $\vec{m} = \vec{m}_0(\theta, \varphi)$. Using perturbation theory in the parameters K_s/J [23, 24, 30], it is possible to calculate effective anisotropy of multi-spin nanoparticles with Néel surface anisotropy term as effective macro-spins. It has been shown that in symmetric nanoparticles such as spheres the uniaxial contribution to the anisotropy vanishes and the next order cubic contribution becomes the dominant one. In agreement with theoretical predictions the landscapes can be fitted to the effective macro-spin energy:

$$\mathcal{E}_{\text{EOSP}} = -K_{\text{ua}}^{\text{eff}} m_z^2 - \frac{1}{2} K_{\text{ca}}^{\text{eff}} (m_x^4 + m_y^4 + m_z^4), \quad (7)$$

where $K_{\text{ua}}^{\text{eff}}$ and $K_{\text{ca}}^{\text{eff}}$ are the effective uniaxial and cubic anisotropy constants. Note that these should not be confused with $K_{\text{eff}}(K_{\text{ua}}^{\text{eff}}, K_{\text{ca}}^{\text{eff}}) = \Delta E/V$. The relevant energy barrier separating well-defined minima can therefore be calculated from the effective energy landscape.

Figure 1 shows a typical plot of the energy surface for a spherical nanoparticle with uniaxial anisotropy cut from a sc crystal. The energy is plotted as a function of the constraint angle θ for two values of the constraint angle $\varphi = 0, \pi/4$ and the strength of the surface anisotropy $K_s = 10K_c, 50K_c, 100K_c$ (for typical Co parameters and a spherical nanoparticle with a diameter of 7.8 nm the value $K_s = 10K_c$ would correspond to approximately 0.63 erg cm $^{-2}$). The onset of an additional cubic anisotropy is clearly seen as a change in the value of the local maximum energy at $\varphi = \pi/4$ (the saddle point) and $\varphi = 0$ (the absolute maximum). For the largest value of the surface anisotropy $K_s = 100K_c$, the energy landscape has predominantly cubic form, characterized by a four-fold anisotropy. The effective uniaxial and cubic anisotropy constants can be extracted from these figures by fitting the curves to equation (7). The surface introduces an additional cubic anisotropy with $K_{\text{ca}}^{\text{eff}} < 0$ for spherical particles cut from a sc crystal lattice and $K_{\text{ca}}^{\text{eff}} > 0$ for those with an fcc crystal structure. The same is true for the truncated octahedron, although depending on the orientation of the facets [31], an additional cubic constant $K_{2,\text{ca}}^{\text{eff}}$ may be required for the fitting.

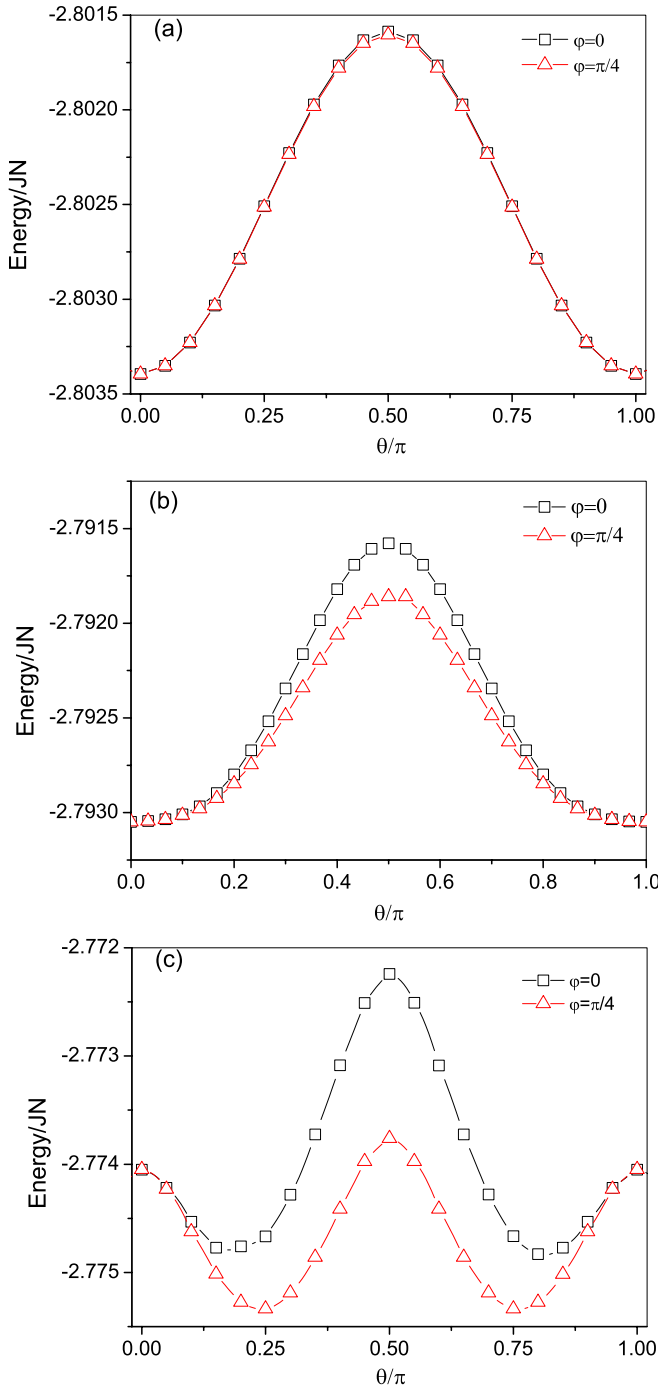


Figure 1. Internal energy for $T = 0$ K for $\varphi = 0$ and $\varphi = \pi/4$ as a function of the constraint angle θ in a spherical nanoparticle with uniaxial anisotropy in the core, sc internal structure ($N = 6272$, $N_c = 4968$ and $N_s = 1304$) for three values of the Néel surface anisotropy $K_s = 10K_c$, $50K_c$, $100K_c$ (from top to the bottom graphs).

The recently developed CMC method [34] is a Monte Carlo (MC) algorithm which allows the inclusion of both thermodynamic fluctuations and entropy into the evaluation of macroscopic quantities, such as temperature-dependent magnetic anisotropy. The MC moves are constructed so that the direction of the average magnetization $\vec{m}_0(\theta, \varphi)$ is fixed while allowing its absolute value to change fully according to

the Boltzmann distribution. Specifically the method acts on two spins for each move, forcing the motion of a second spin to correct for the motion of the first, such that the direction of the average magnetization is conserved. The moves are constructed in such a way that both reversibility and ergodicity are naturally preserved.

When dealing with temperature dependent effects one is concerned with the Helmholtz *free* energy of the system, $\mathcal{F} = \mathcal{H} - TS$, rather than just the internal energy, \mathcal{H} . This presents a significant problem since in general free energies are difficult to calculate and the Hamiltonian only gives the internal energy explicitly. However, it has been shown [34] that the free energy can be recovered (by integration) from the thermodynamic average of the torque, given by

$$\mathcal{T} = \left\langle - \sum_i [\vec{s}_i \times \partial \mathcal{H} / \partial \vec{s}_i] \right\rangle. \quad (8)$$

For the case where the only anisotropic contribution to the Hamiltonian comes from the magnetocrystalline anisotropy (as opposed to anisotropic exchange, for example), and the functional form of the torque is known analytically, it is possible to calculate the free energy simply by calculation of the derivative (i.e. the torque). In our case, it is known that the system will possess only cubic or uniaxial components, and so by calculating the torque on the system the free energy is also known. By variation of the constraint angles the anisotropic free energy can be recovered. For the case of $\varphi = 0$, the simulated angular dependence of the y -component of the torque is then fitted to

$$\mathcal{T}_y(\theta) = -K_{ua}^{\text{eff}}(T) \sin(2\theta) - \frac{1}{2} K_{ca}^{\text{eff}}(T) \sin(4\theta). \quad (9)$$

Figure 2 presents the results for the Y -component of the average restoring torque for the nanoparticles whose energy zero-temperature landscapes are presented in figure 1. The shapes of the torque curves are well described by expression (9) for all temperatures with the effective anisotropy constants decreasing with temperature. For relatively small strength of the surface anisotropy $K_s = 10K_c$, only uniaxial anisotropy is present. For the larger value of the anisotropy constant $K_s = 100K_c$ we observe the competition of two anisotropies: uniaxial and additional cubic due to surface effects. At high temperatures, however, the cubic anisotropy contribution disappears.

3. Results

We have carried out a systematic investigation of the effects of surface anisotropy on the energy surface and effective anisotropy of the model nanoparticles using the CMC method.

The torque curves, such as those presented in figure 2, allow the investigation of the temperature dependence of the effective anisotropies in nanoparticles. Specifically, the torque curves are analysed at each temperature to determine the uniaxial and cubic contributions, whose individual temperature dependence can be calculated. Figure 3 presents the corresponding temperature dependence of uniaxial and

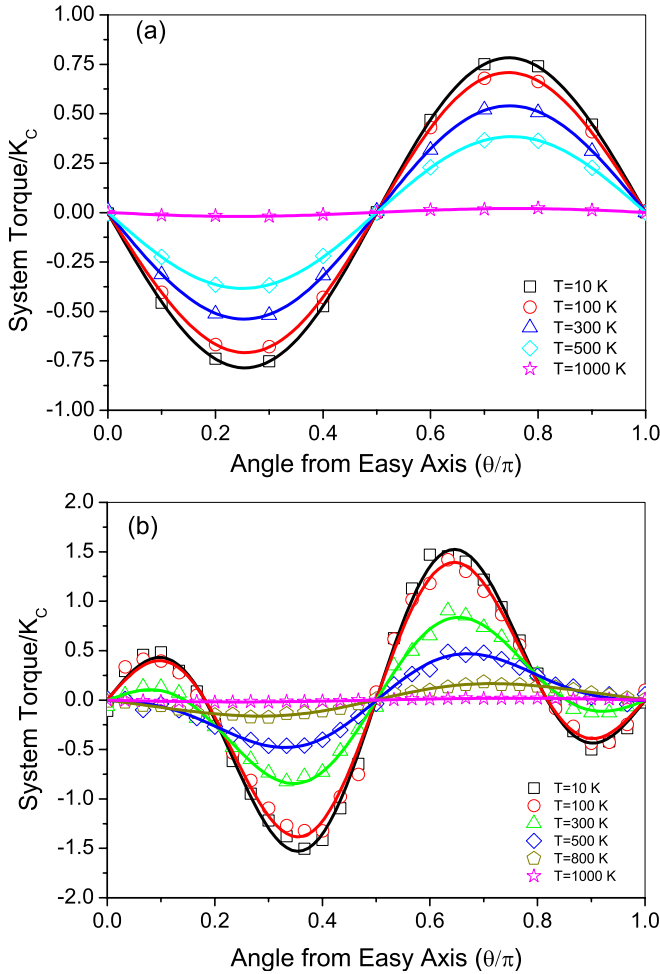


Figure 2. The Y-component of the torque for $\varphi = 0$ as a function of the constrained angle θ for various temperatures in a spherical nanoparticle with uniaxial anisotropy in the core, sc crystal structure ($N = 6272$, $N_C = 4968$ and $N_S = 1304$) and two values of the Néel surface anisotropy (a) $K_s = 10K_c$ and (b) $K_s = 100K_c$. The line is a fitting curve to equation (9).

additional cubic anisotropy for the two values of the surface anisotropy constant. The uniaxial anisotropy is independent of the surface anisotropy value, as expected. The cubic anisotropy, coming from the surface anisotropy, is practically zero for small strength of the surface anisotropy $K_s = 10K_c$. In the case of strong surface anisotropy $K_s = 100K_c$ this additional cubic anisotropy is negative and its absolute value decreases with temperature. As is the case with bulk cubic anisotropy, the surface-induced cubic anisotropy has a stronger temperature dependence compared with the uniaxial core contribution. Consequently, at high temperatures the cubic counterpart disappears leaving the uniaxial core anisotropy as the dominant factor. A transition in the magnetic behaviour then can take place. A similar phenomenon is observed in thin films with strong surface effects: at low temperatures the surface effects predominate and the magnetization of the film is perpendicular to the thin film plane, while at higher temperatures the surface anisotropy vanishes and the magnetization re-orientates in-plane. In the case of nanoparticles a similar effect occurs: at low temperatures the surface effects dominate giving rise to cubic behaviour, while

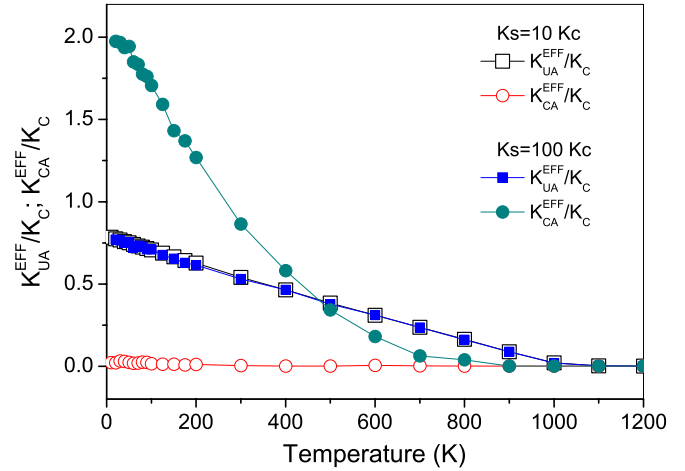


Figure 3. Temperature dependence of anisotropies in a spherical nanoparticle with uniaxial anisotropy in the core, sc internal structure ($N = 6272$, $N_C = 4968$ and $N_S = 1304$) and two values of the Néel surface anisotropy $K_s = 10K_c$ and $K_s = 100K_c$. The values are normalized by the core anisotropy K_c . The value of $K_{UA}^{EFF}/K_C < 1$ at $T = 0$ due to the fact that the surface atoms have surface anisotropy only.

at high temperatures the surface contribution vanishes and the nanoparticle exhibits a uniaxial anisotropy.

In the case of nanoparticles with cubic core anisotropy, the surface anisotropy induces an additional contribution which is also cubic in nature, with the sign of the anisotropy dependent on the crystal symmetry. Specifically, the cubic surface anisotropy constant is positive for nanoparticles cut from an fcc lattice and negative for those cut from a sc lattice. The contribution of the surface-induced anisotropy is additive to the bulk value, although one should note [23, 24, 31] that it is proportional to K_s^2 , rather than to K_s . Examples of the average torque curve are plotted in figure 4 for various temperatures. The shape of the curves remains consistent with the free energy surface expected for cubic anisotropy for all temperatures and surface anisotropy values. Thus, the cubic anisotropy arising from the surface contribution is apparently indistinguishable from the bulk. However, there is an important distinction in terms of the scaling behaviour of the two contributions, as will be discussed later.

In figure 5 we present the effective cubic anisotropy constant in a truncated octahedral nanoparticle cut from an fcc crystal structure for various values of the Néel surface anisotropy constant. The appearance of an additional positive cubic anisotropy contribution coming from the surface is seen for values of $K_s \gtrsim 20K_c$. The low-temperature values of the effective anisotropy coincide with those obtained through the Lagrange multiplier technique at $T = 0$ K. In figure 6 we present the temperature dependence of the total cubic anisotropy in spherical and truncated octahedral nanoparticles with fcc internal structures and for various values of the Néel surface anisotropy K_s . These values are normalized by the value of the effective anisotropy at $T = 0$ K (K_{ca}^{eff}) which is different for each case. A universal temperature dependence of the overall cubic anisotropy, independent on its value at $T = 0$ K, is observed.

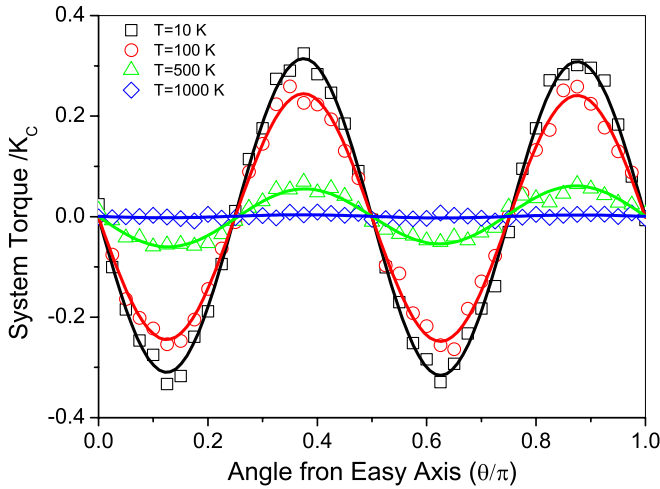


Figure 4. Angular dependence of the Y -component of the total system torque in a truncated octahedral nanoparticle with fcc crystal structure ($N = 1289$, $N_C = 482$ and $N_S = 807$), Néel surface anisotropy $K_s = 20K_c$ and various values of the temperature.

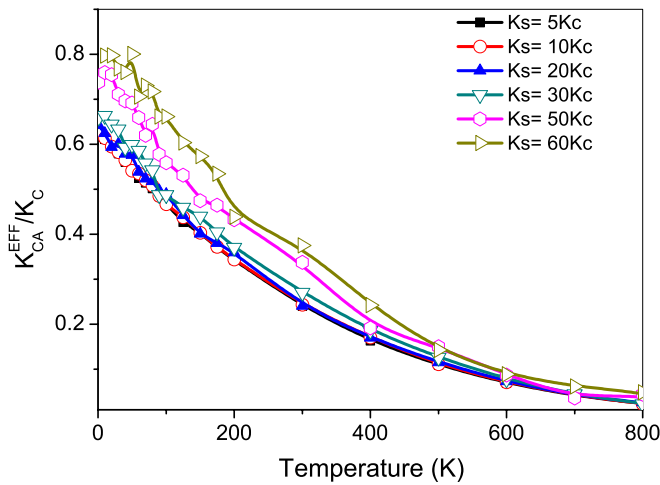


Figure 5. Temperature dependence of the effective cubic anisotropy, normalized to the core anisotropy value in truncated octahedra nanoparticles with cubic anisotropy in the core, fcc crystal structure ($N = 1289$, $N_C = 482$ and $N_S = 807$) and various values of the Néel surface anisotropy.

Figure 7 presents the dependence of the effective anisotropy on the value of the surface anisotropy K_s for various temperatures for truncated octahedra cut from an fcc lattice with cubic anisotropy in the core. As for a previous case, the surface anisotropy contribution is of the same cubic nature as the core one, and the additional surface contribution is expected to be proportional to K_s^2 , see [23, 24]. Consequently, all the data were fitted to this theoretically predicted dependence. The extracted values $K_c^{\text{eff}}(T)$ are consistent with those calculated independently. The corresponding formula $K_{\text{eff}}(T) = K_c^{\text{eff}}(T) + AK_{\text{Surf}}(T)$ ($K_{\text{Surf}}(T) \sim K_s^2$) may be viewed as a substitution for the original formula (1). Unfortunately, the system size dependence of the A parameter is not trivial [23, 24], since it depends on the surface density of spins. The latter is not a smooth function of the nanoparticle diameter, due to the fact that small nanoparticles do not have uniform spin density on their surfaces.

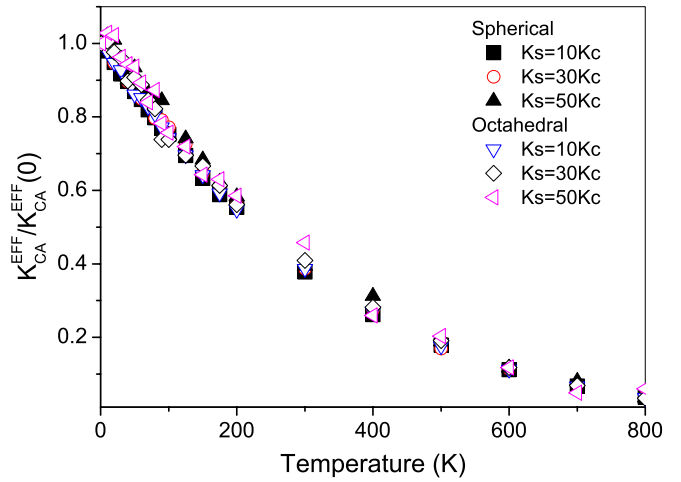


Figure 6. Temperature dependence of the effective cubic anisotropy, normalized to its value at $T = 0$ K in spherical ($N = 1505$) and truncated octahedra (the same as in figure 5) nanoparticles with cubic anisotropy in the core, fcc crystal structure and various values of the Néel surface anisotropy.

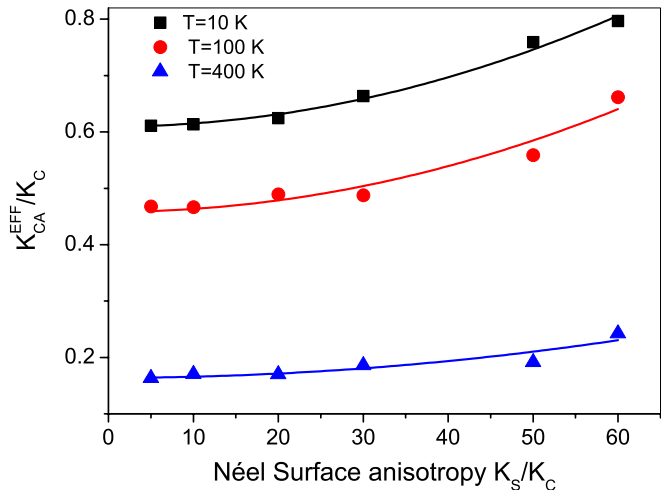


Figure 7. The effective cubic anisotropy as a function of the Néel surface anisotropy parameter in a truncated octahedral nanoparticle (the same as in figure 5) with cubic anisotropy in the core, fcc crystal structure and for various temperatures.

Finally, we discuss the scaling behaviour of the effective anisotropy on the nanoparticle magnetization $K \propto M^\gamma$. The Callen–Callen theory [35] states that at low temperatures in the bulk $\gamma = 3$ and 10 for uniaxial anisotropy and cubic anisotropy, respectively. For nanoparticles, the surface magnetization has a faster temperature dependence than the core, as shown in figure 8, sharing the same Curie temperature, T_c . This arises due to a reduction in coordination number at the surface leading to a reduced exchange and a strong surface anisotropy pointing perpendicularly to the surface. At the same time the fully coordinated core effectively polarizes the surface layer, resulting in a shared value for T_c . The surface anisotropy value has very little effect on the temperature dependence of the overall anisotropy, as shown in figure 6. The total effect is that the scaling exponents are always smaller than the corresponding bulk value and decreases with the surface anisotropy value. For example, in figure 9 we present the scaling of the uniaxial and

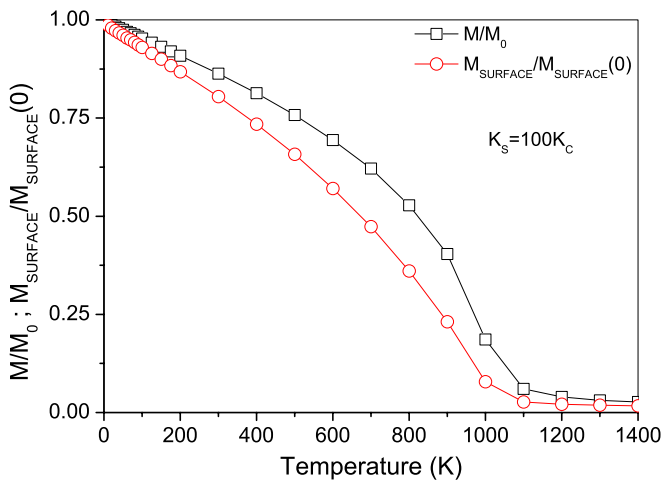


Figure 8. Temperature dependence of core and surface magnetization, normalized to $T = 0$ K values in a spherical nanoparticle ($N = 1505$) with sc lattice.

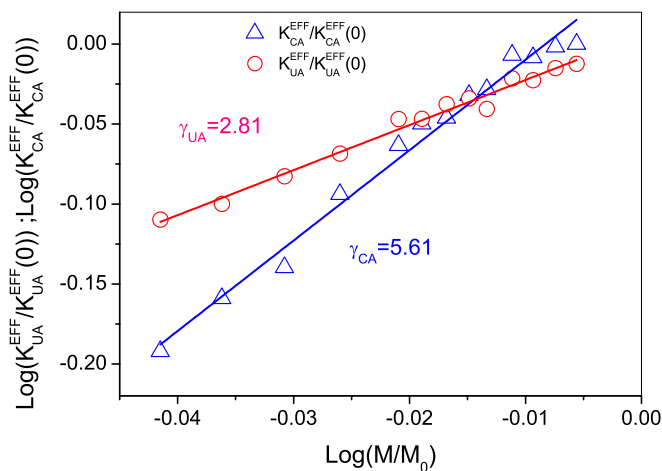


Figure 9. Low-temperature scaling of the effective anisotropies with magnetization in a spherical nanoparticle cut from a sc crystal lattice, uniaxial anisotropy and Néel surface anisotropy parameter $K_s = 100K_c$.

cubic anisotropy constants with the magnetization at low temperatures up to 200 K in a spherical nanoparticle with uniaxial core anisotropy. Note that no scaling behaviour is observed in the whole temperature range.

A similar effect is observed in spherical and truncated octahedral nanoparticles with cubic core anisotropy. In figure 10 we present the scaling exponent as a function of Néel surface anisotropy constant in nanoparticles with spherical and octahedral shapes, fcc crystal structure and cubic anisotropy in the core. As with the uniaxial core anisotropy, the scaling exponents are also lower than the corresponding bulk values and weakly depend on the surface anisotropy value. In fact, the scaling exponent decreases as a function of the surface anisotropy value due to a faster decrease in the magnetization on the surface.

4. Conclusions

By means of the recently developed CMC method, we have been able to evaluate the temperature dependence of magnetic

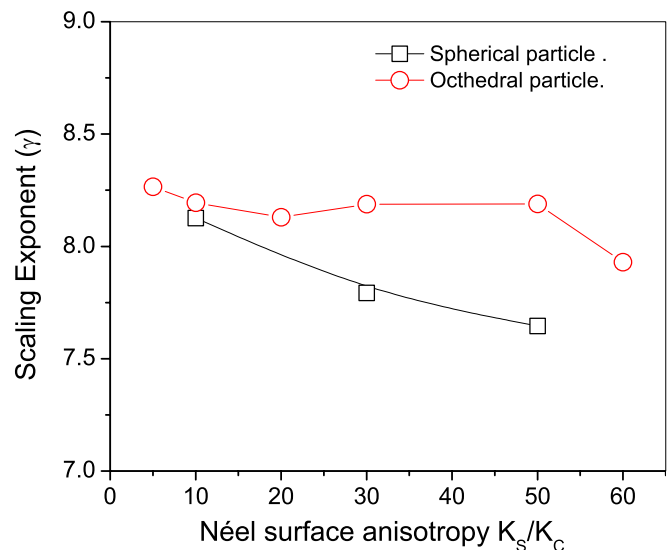


Figure 10. Scaling exponents as a function of Néel surface anisotropy constant in spherical ($N = 1505$) and truncated octahedra ($N = 1289$) nanoparticles with cubic anisotropy in the core and fcc internal structure.

anisotropies in nanoparticles with different shapes and internal structures. An additional cubic anisotropy, due to the spin nonlinearities produced by the surface anisotropy, was reported earlier in a series of works at $T = 0$ K [23, 24, 30]. This effect is shown to persist when temperature is included.

We have calculated the temperature dependence of uniaxial and cubic anisotropy contributions. The additional cubic anisotropy shows a faster dependence on temperature than the uniaxial core anisotropy. Therefore, the temperature-induced transition from the cubic anisotropy to the bulk one can be observed. This effect is similar to the reorientation transition in thin films. It has a purely surface origin and it is independent of the structural changes which may occur in nanoparticles with temperature. In nanoparticles with cubic core anisotropy, the surface contribution is additive and increases or decreases the value of the overall anisotropy. The temperature dependence of the total cubic anisotropy is universal and only weakly dependent on the value of the surface anisotropy. The scaling exponent of the anisotropy with magnetization depends on the surface anisotropy value and is always lower than the bulk scaling exponent due to strong magnetization fluctuations at the surface.

Acknowledgments

This work has been supported by the grants MAT2007-66719-C03-01 and CS2008-023 from the Spanish Ministry of Science and Innovation and also from EC FP7 Grants No NMP3-SL-2008-214469 (UltraMagnetron) and No 214810 (FANTOMAS). The financial support from the European COST P-19 Action is also gratefully acknowledged.

References

- [1] Lu A-H, Salabas E L and Schüth F 2007 *Angew. Chem. Int.* **46** 1222

- [2] Tartaj P *et al* 2005 *J. Magn. Magn. Mater.* **290–291** 28
- [3] Fiorani D (ed) 2005 *Surface Effects in Magnetic Nanoparticles* (New York: Springer)
- [4] Salazar-Alvarez G *et al* 2008 *J. Am. Chem. Soc.* **130** 13234
- [5] Paz E, García-Sánchez F and Chubykalo-Fesenko O 2008 *Physica B* **403** 330
- [6] Skumryev V *et al* 2003 *Nature* **423** 850
- [7] Evans R F L *et al* 2009 *Europhys. Lett.* **88** 57004
- [8] Luis F *et al* 2002 *Phys. Rev. B* **65** 094409
- [9] Bartolomé J *et al* 2008 *Phys. Rev. B* **77** 184420
- [10] Luis F *et al* 2006 *Europhys. Lett.* **76** 142
- [11] Sun S *et al* 2000 *Science* **287** 1989
- [12] Garcia-Sanchez F *et al* 2008 *J. Appl. Phys.* **103** 07F505
- [13] Aranda G R *et al* 2009 *J. Appl. Phys.* **105** 07B514
- [14] Jamet M *et al* 2004 *Phys. Rev. B* **69** 24401
- [15] Dorfbauer F *et al* 2007 *J. Magn. Magn. Mater.* **316** E791
- [16] Evans R *et al* 2007 *IEEE Trans. Magn.* **43** 3106
- [17] Binns C *et al* 2002 *J. Phys.: Condens. Matter* **318** 350
- [18] Bodker F, Mörup S and Linderöth S 1994 *Phys. Rev. Lett.* **72** 282
- [19] Goya G F *et al* 2003 *J. Appl. Phys.* **94** 3520
- [20] Pérez N *et al* 2008 *Nanotechnology* **19** 475704
- [21] Xie Y and Blackman J A 2004 *Phys. Rev. B* **69** 172407
- [22] Xie Y and Blackman J 2004 *J. Phys.: Condens. Matter.* **16** 3163
- [23] Garanin D A and Kachkachi H 2003 *Phys. Rev. Lett.* **90** 065504
- [24] Yanes R *et al* 2007 *Phys. Rev. B* **76** 064416
- [25] Berger L *et al* 2008 *Phys. Rev. B* **77** 104431
- [26] Mazo-Zuluaga J *et al* 2009 *J. Appl. Phys.* **105** 123907
- [27] Kachkachi H and Mahboub H 2004 *J. Magn. Magn. Mater.* **278** 334
- [28] Néel L 1954 *J. Phys. Radium* **15** 376
- [29] Victora R H and MacLaren J M 1993 *Phys. Rev. B* **47** 11583
- [30] Kachkachi H and Bonet E 2006 *Phys. Rev. B* **73** 224402
- [31] Yanes R and Chubykalo-Fesenko O 2009 *J. Phys. D: Appl. Phys.* **42** 055013
- [32] Jamet M *et al* 2001 *Phys. Rev. Lett.* **86** 4676
- [33] Kachkachi H and Schmool D S 2007 *Eur. J. Phys. B* **56** 27
- [34] Asselin P *et al* 2010 *Phys. Rev. B* **82** 054415
- [35] Callen H B and Callen E 1966 *J. Phys. Chem. Solids* **27** 1271